

Deformation mechanisms and pseudoelastic behaviors in trilayer composite metal nanowires

N. Abdolrahim, I. N. Mastorakos, and H. M. Zbib

School of Mechanical and Materials Engineering, Washington State University, Pullman, Washington 99164, USA

(Received 30 November 2009; revised manuscript received 2 February 2010; published 26 February 2010)

The deformation mechanisms in Cu-Ni-Cu composite nanowires subjected to uniaxial tensile loading are investigated using molecular-dynamics simulations. We particularly explore the coupled effects of geometry and coherent interface on the tendency of nanowires to deform via twins and show pseudoelastic behavior. It is found that the critical size to exhibit pseudoelasticity in composite nanowires is $5.6 \times 5.6 \text{ nm}^2$, which is 6.5 times greater than single-crystalline Cu nanowires. Our results also show that the composite nanowires offer stiffness enhancement compared to the corresponding single-crystal Cu nanowires.

DOI: [10.1103/PhysRevB.81.054117](https://doi.org/10.1103/PhysRevB.81.054117)

PACS number(s): 62.25.-g, 61.46.-w, 68.65.-k

I. INTRODUCTION

Nanowires are regarded among the most important nanometer materials¹⁻³ because of their distinctive structures and properties that can play a critical role in future electronic, optical, and nanoelectromechanical systems.^{4,5} Nanowires are typically single-crystalline, highly anisotropic, and semi-conducting, insulating or metallic nanostructures that result from rapid growth along one direction. Their cross-section is uniform and much smaller than their length. The result of this is a very high surface to volume ratio, causing the surface atoms to contract toward the core of nanowire in order to minimize their energy by maximizing their local electron density. The surface contradiction results into very high compressive stresses in the nanowires, affecting significantly their mechanical behavior during tensile loading. When the cross-sectional area of single-crystal metallic nanowires made of Cu, Ni, and Au is smaller than a critical value, the wires can completely recover from severe deformations, up to 50% strains, in a very short response time without inducing residual deformation.⁶⁻¹⁰ Their unique pseudoelastic behavior, which is very important in the area of self-healing materials used as sensors for bioengineering applications and microelectronics, only exists in nanowires of face-centered-cubic (fcc) metals with high twinnability. This size-dependent pseudoelastic behavior is mainly due to the surface-induced internal compressive stress in nanowires, in the order of gigapascal, which is much higher than in bulk materials and provides the driving force for spontaneous lattice reorientation via twins.⁶ However, measuring the mechanical properties of nanowires is a very difficult task due to their small dimensions. Molecular-dynamics (MD) simulations provide a useful tool to investigate the structural, mechanical, and thermodynamic properties of these nanoscale materials at the atomic level. Various investigations have been done on single-crystalline nanowires and their behaviors.⁶⁻¹⁰ In the present work we particularly use MD to study deformation mechanisms in composite nanowires and compare their behavior to single-crystalline nanowires.

II. DEFORMATION MECHANISMS IN NANOWIRES

Previous studies have shown that in defect-free fcc single-crystalline nanowires made of Cu, Ni, and Au, when de-

formed at strain rate below a critical value,¹ the deformation behavior is driven by the nucleation of $1/6\langle 112 \rangle$ -type dislocation partials at the surface; and whether full type dislocations or twins are formed depends on the stacking fault energy, surface effects, and the size of the nanowire.¹¹⁻¹⁵ During tensile loading, at a critical-resolved shear stress a leading $1/6\langle 112 \rangle$ partial dislocation nucleates at the surface and propagates in the nanowires. For sizes larger than a critical value, a trailing partial emits on the same plane resulting in the formation of a full dislocation and leading to permanent deformation (slip). Below the critical dimension, a second leading partial nucleates at a slip plane adjacent to the original slip plane, resulting in the formation of a twin boundary. The process of emission of partials repeats itself and moves the twin boundary along the axis of the wire. At sizes lower than the temperature-dependent critical size, an initial configuration with $\langle 001 \rangle$ axis and $\{001\}$ lateral surfaces is unstable due to high surface energies which cause the crystalline structure to undergo spontaneous reorientation to a low-energy configuration of $\langle 110 \rangle$ axis and $\{111\}$ closed-packed lateral surfaces. The reoriented $\langle 110 \rangle / \{111\}$ wires are found to exhibit pseudoelasticity upon application and subsequent removal of tensile loading.⁶ The pseudoelastic behavior occurs only above a size-dependent critical temperature T_{cr} . For a given wire size if the unloading takes place at temperatures below T_{cr} , the reversible behavior does not occur, leaving the question as to why is the temperature important for the pseudoelastic process. The answer is related to the energetic barrier and the driving force. To initiate the deformation, partial dislocations nucleate and propagate to accommodate high-energy mobile twin boundaries, which constitute an energy barrier for the reversibility of the deformation. Thermal energy can provide the necessary energy for overcoming the barrier. As the wire size increases the surface-induced compressive stress σ decreases and, above a critical size, can no longer activate the recovery process. Therefore higher temperatures or external compressive stresses are needed to initiate the reverse process. This size and temperature dependence has been observed in experiments as well as in atomistic simulations.^{11,16} At room temperature the critical size beyond which the nanowires exhibit pseudoelastic behavior is $1.8 \times 1.8 \text{ nm}^2$ (5×5 crystal lattice units) for Cu and $1.061 \times 1.061 \text{ nm}^2$ (3×3 crystal lattice units) for Ni. This behavior is attributed to the high twinnability that these two materials exhibit among the fcc

metals.^{6,13} It should be pointed out that the critical dimensions mentioned above correspond to the initial unstable configurations with $\langle 001 \rangle$ orientation, which reorient to stable $\langle 110 \rangle$ configurations whose dimensions are $2.19 \times 2.19 \text{ nm}^2$ for Cu and $1.6 \times 1.6 \text{ nm}^2$ for Ni.

For many practical applications, and from manufacturability point of view, it is desirable to increase the critical size for pseudoelasticity. Previously Ji and Park^{16,17} showed that by simply changing the wire cross-section from square to rectangle, nanowires with dominant surface facets are created with increased tendency to deform via twinning. Since the twinning is the mechanism responsible for the pseudoelastic behavior, this leads to increased critical size. It is suggested that the asymmetry of the cross-sectional geometry of each layer results in an additional driving force for the larger surfaces to reduce their area and therefore their energy by forming twins. Another driving force that can increase the critical size is the addition of internal stresses that result when creating fcc/fcc composite nanowires with coherent interfaces.^{18–21} Within a composite nanowire, made of a Ni layer sandwiched between two Cu layers, the resulting coherency stresses will add to the already existing surface stresses, thus enhancing the driving force and causing the nanowire to exhibit pseudoelastic behavior at cross-sectional areas larger than the critical value for a single-crystalline nanowire. At this juncture it is worth mentioning that it is possible to fabricate nanowires the by creating thin films using already established techniques such as sequential sputtering,¹⁸ electrodeposition,^{22,23} or electron-beam lithography and then thinning them in appropriate dimensions through focus ion beam (or reactive-iron etching).²⁴ In this work, the coupled effects of rectangular geometry and coherent interface on increasing the critical size of nanowires to exhibit pseudoelastic behavior are presented and discussed.

III. MOLECULAR-DYNAMICS SIMULATIONS

The MD simulations were performed using LAMMPS (Ref. 25) with potentials based on the embedded atom method.^{26,27} All simulations were achieved with free surfaces. Composite nanowires were created with surface orientations along $\langle 11\bar{2} \rangle$, $\langle 111 \rangle$, and $\langle 1\bar{1}0 \rangle$, i.e., x , y , and z . The temperature of the structure during all the stages of the simulation (relaxation, loading, and unloading) was kept constant at 300 K. Initially the nanowires were not in equilibrium. They were relaxed keeping the bottom fixed on its plane and the top free to move without applying any load until the final strain of the nanowires reached a steady state. The relaxed nanowires were then subjected to a uniaxial tensile loading by pulling the top by a constant velocity, thus simulating constant strain rate loading conditions. The velocity during all the simulations was kept constant and equal to 0.03 \AA ps^{-1} that corresponds to the strain rate of 10^8 s^{-1} , which is at least two orders of magnitude smaller than the critical strain rate (around $5 \times 10^{10} \text{ s}^{-1}$) for the initiation of amorphization during the tensile loading.¹ After the desired strain was achieved, the nanowires were unloaded by simply implementing negative velocity of $-0.03 \text{ \AA ps}^{-1}$.¹³ It should be mentioned that the atoms of top surface are constrained to

TABLE I. Cross-sectional dimensions of simulated Cu-Ni-Cu composite nanowires. The units are in nanometer.

Case	Overall size	Cu layer	Ni layer
1	2.4×2.4	0.8×2.4	0.8×2.4
2	2.8×2.8	0.93×2.8	0.93×2.8
3	3.54×3.54	1.18×3.54	1.18×3.54
4	4.17×4.17	1.39×4.13	1.39×4.13
5	4.8×4.8	1.6×4.8	1.6×4.8
6	5.24×5.24	1.82×5.24	1.6×5.24
7	5.6×5.6	2×5.6	1.6×5.6

move only along the wire axis by applying velocity in the vertical direction during the loading and unloading periods; they are not free to move in the other two directions. The cross-sectional dimensions of the simulated nanowires as well as the size of each single layer are given in Table I.

IV. RESULTS AND DISCUSSION

The stress-strain curves of a composite nanowire together with the same size Cu nanowire under tensile loading are shown in Fig. 1. It is noticed that the presence of the coherent interface results in an increase in the yield stress from 4.2 GPa in the monolithic $2.4 \times 2.4 \text{ nm}^2$ Cu nanowire to 5.28 GPa in the same size Cu-Ni-Cu composite nanowire. This is attributed to the coherency compressive stress exerted in the Cu layers in addition to the surface compressive stress, thus increasing the initial stored strain energy and resulting in higher tensile stresses when loading the wire in tension starting from the compressive state. As can be deduced from Fig. 1, in both cases, fracture starts at strain of about 40% followed by rapid drop in the stress. It should be noted that in the case of single-crystalline nanowires we compared our results in Fig. 1 with similar results found in the literature¹¹ using the same potential²⁸ but different computational approach and the results are similar.

The nanowires that correspond to the first five cases (layers with the same thickness) of Table I exhibit very good

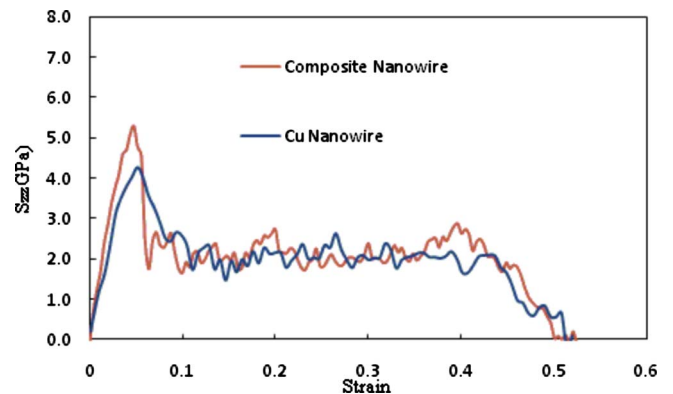


FIG. 1. (Color online) Comparison of the stress-strain curve for a $\{110\}/\{111\}$ $2.4 \times 2.4 \text{ nm}^2$ composite Cu-Ni-Cu nanowire with the same size single-crystalline nanowire at the temperature of 300 K.

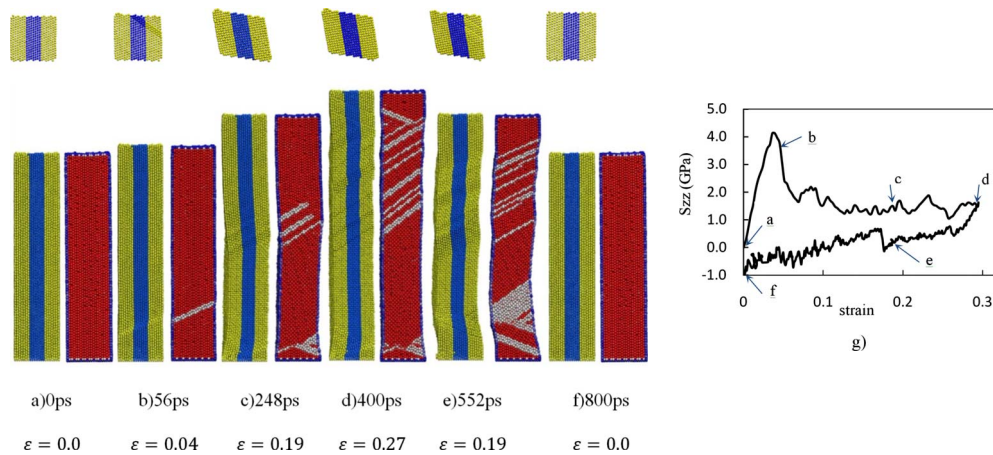


FIG. 2. (Color online) Steps (a)–(f) show the snapshots of $4.17 \times 4.17 \text{ nm}^2$ composite nanowire with the original configuration of $\langle 110 \rangle / \{111\}$ during loading and unloading at the temperature of 300 K accompanied with their matching section view according to the centrosymmetry parameter. Curve (g) shows the corresponding stress-strain curve.

pseudoelastic behavior as can be seen in Fig. 2 for case 4. Figures 2(a)–2(f) show the reorientation process in a $4.17 \times 4.17 \text{ nm}^2$ trilayer composite nanowire during loading and unloading at different snapshots together with the section views of the same nanowire according to centrosymmetry parameter. The first twin boundary forms at the strain of 0.039 and as loading is continued it moves along the wire axis and thus changes the original configuration of $\langle 110 \rangle / \{111\}$ to the new configuration of $\langle 001 \rangle / \{001\}$. This new configuration is not in a stable mode due to the high surface energies. Therefore, upon unloading the unstable $\langle 001 \rangle / \{001\}$ nanowire then reorients back to its original low energy state of $\langle 110 \rangle / \{111\}$ configuration. As it can be seen from the figures, due to the complete coherent interface the twin boundaries traverse the three layers and propagate along the wire axis upon loading and unloading. Since Cu and Ni are in fcc phase, the centrosymmetry contour shows both of them with the same color. Also because of no phase transformation during the reorientation process, there is no color change between the two configurations of $\langle 110 \rangle / \{111\}$ and $\langle 001 \rangle / \{001\}$; both are fcc. Figure 2(g) shows the resulting stress-strain curve.

Unlike the solid nanowires in which the twins initiate from the sharp edges of free surfaces, in composite nanowires the first twin boundary initiates from the free surface at the interface between Cu and Ni and propagates first in the Ni layer and afterwards expands to the neighboring Cu layers. The reason is that the Ni layer is under high internal coherent tensile stress which makes it easier to overcome the stress barriers to initiate the twin, Fig. 3.

The simulation results show that by increasing the thickness of the Ni layer beyond 1.6 nm (which is the critical thickness for single-crystalline Ni nanowire) the nanowire starts to fracture after the yield point and no twinning occurs. However, the width of each layer can be increased far beyond this critical thickness, e.g., it is 4.17 nm in case 5. Therefore, the thickness of the Ni layer was kept at the critical size of 1.6 nm and in the next two cases the thickness of each layer of Cu layers increased up to 2 nm, below which the nanowires exhibit pseudoelastic behavior. Beyond the

stated thickness, fracture initiates at the primary steps of loading due to the growth of the tensile stress in Ni and reduction of both surface and coherent compressive stress in the Cu layers, which contributes to the generation of full dislocations instead of twins.

In Table II we summarize the yield properties of the composite nanowires of the different sizes at the temperature of 300 K. Since smaller wires have higher surface-to-volume ratios, they have higher strain energies and consequently are stronger than larger wires. Therefore, by increasing the size of the wire the yield stress decreases. Although the overall behavior of the composite nanowires is comparable to single-crystalline nanowires, the composite nanowires have

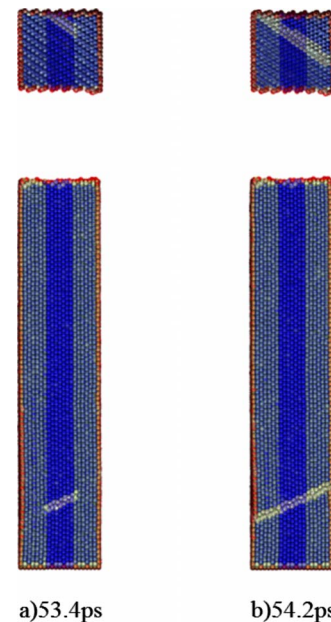


FIG. 3. (Color online) Snapshot of overlapping both the geometry of nanowire and the related centrosymmetry parameter simultaneously exactly after the initiation of the first twin at the strain of $\epsilon = 0.039$. The top pictures show the cross-sectional view and the bottom the side view.

TABLE II. Yield parameters of simulated pseudoelastic Cu-Ni-Cu composite nanowires at $T=300$ K.

Case	Wire size	ϵ_y	σ_y (GPa)
1	2.4×2.4	0.048	5.28
2	2.8×2.8	0.056	5.09
3	3.54×3.54	0.05	5.01
4	4.17×4.17	0.039	4.13
5	4.8×4.8	0.045	4.38
6	5.24×5.24	0.038	4.1
7	5.6×5.6	0.044	4.12

higher yield stress when compared to similar monolithic Cu nanowires (Fig. 1). The interesting result is that even composite nanowires with larger size of 3.54×3.54 nm² have higher yield stresses than the 2.4×2.4 nm² Cu nanowire. Since the temperature is a key parameter in pseudoelastic behavior of nanowires, by varying the temperature the results shown in Table II will change. Also we investigated the effect of strain rate within the range of $10^7 - 10^9$ s⁻¹. The result shows that there is an effect on the yield properties, as expected, but not on the pseudoelastic behavior, Fig. 4. We also performed analysis under quasistatic loading conditions and the results show that the pseudoelastic behavior does not change although there is a significant drop in the yield stress. These results are not surprising since the pseudoelastic behavior is driven by surface and coherency stresses while the yield stress can be strain rate dependent.

Figure 4 shows the stress-strain curve for the composite nanowire with the critical size of 5.6×5.6 which still shows good pseudoelasticity. Increasing the size of the wire beyond this critical size leads to the formation of full dislocations instead of the initiation and propagation of twins across the wire axis.

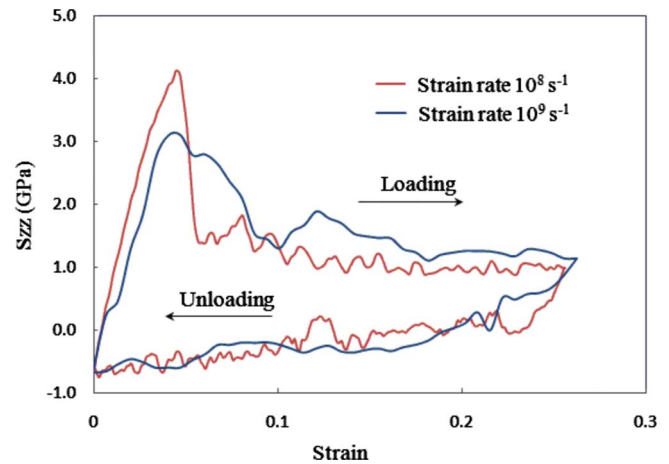


FIG. 4. (Color online) Stress-strain curve of a $\langle 110 \rangle / \{111\}$ 5.61×5.63 nm² composite nanowire during loading and unloading at the temperature of 300 K.

V. CONCLUSIONS

In conclusion by utilizing molecular-dynamics simulations, we have shown that below a critical-size composite trilayer nanowires deform via twinning and exhibit pseudoelastic behavior. We have shown that because of the coupled effects of coherent interface and rectangular geometry of layers, the critical size is 6.5 times greater than that for single-crystalline Cu nanowires. Moreover the composite nanowires have higher yield stresses than similar single-crystalline nanowires which indicate that composite nanowires also offer stiffness enhancement compared to the corresponding monolithic Cu nanowires.

ACKNOWLEDGMENT

This work was supported by the U.S. Department of Energy under Grant No. DE-FG02-07ER46435.

¹H. Ikeda, Y. Qi, T. Cagin, K. Samwer, W. L. Johnson, and W. A. Goddard, *Phys. Rev. Lett.* **82**, 2900 (1999).
²C. M. Lieber, *Sci. Am.* **285**, 58 (2001).
³J. Hu, T. W. Odom, and C. M. Lieber, *Acc. Chem. Res.* **32**, 435 (1999).
⁴H. G. Craighead, *Science* **290**, 1532 (2000).
⁵K. L. Ekinci and M. L. Roukes, *Rev. Sci. Instrum.* **76**, 061101 (2005).
⁶W. Liang and M. Zhou, *J. Eng. Mater. Technol.* **127**, 423 (2005).
⁷A. Hasmy and E. Medina, *Phys. Rev. Lett.* **88**, 096103 (2002).
⁸F. Ma, S. L. Ma, K. W. Xu, and P. K. Chu, *Appl. Phys. Lett.* **91**, 253114 (2007).
⁹W. Liang and M. Zhou, *Philos. Mag.* **87**, 2191 (2007).
¹⁰H. S. Park, K. Gall, and J. A. Zimmerman, *J. Mech. Phys. Solids* **54**, 1862 (2006).
¹¹W. Liang, D. J. Srolovitz, and M. Zhou, *J. Mech. Phys. Solids* **55**, 1729 (2007).
¹²H. S. Park, K. Gall, and J. A. Zimmerman, *Phys. Rev. Lett.* **95**,

255504 (2005).
¹³W. Liang and M. Zhou, *Phys. Rev. B* **73**, 115409 (2006).
¹⁴X. Guo, W. Liang, and M. Zhou, *Exp. Mech.* **49**, 183 (2009).
¹⁵S. V. Bobylev and I. A. Ovid'ko, *Phys. Rev. Lett.* **103**, 135501 (2009).
¹⁶C. J. Ji and H. S. Park, *Nanotechnology* **18**, 115707 (2007).
¹⁷C. J. Ji and H. S. Park, *Appl. Phys. Lett.* **89**, 181916 (2006).
¹⁸A. Misra, J. P. Hirth, and H. Kung, *Philos. Mag. A* **82**, 2935 (2002).
¹⁹C. H. Henager, Jr., R. J. Kuntz, and R. G. Hoagland, *Philos. Mag.* **84**, 2277 (2004).
²⁰F. Akasheh, H. M. Zbib, J. P. Hirth, R. G. Hoagland, and A. Misra, *J. Appl. Phys.* **101**, 084314 (2007).
²¹I. N. Mastorakos, H. M. Zbib, D. F. Bahr, J. Parsons, and M. Faisal, *Appl. Phys. Lett.* **94**, 043104 (2009).
²²D. E. Kramer and T. Foecke, *Philos. Mag.* **82**, 3375 (2002).
²³C. Bonhote and D. Landolt, *Electrochim. Acta* **42**, 2407 (1997).

- ²⁴C. Vieu, F. Carcenac, A. Pepin, Y. Chen, M. Mejias, A. Lebib, L. Manin-Ferlazzo, L. Couraud, and H. Launois, *Appl. Surf. Sci.* **164**, 111 (2000).
- ²⁵S. Plimpton, *J. Comput. Phys.* **117**, 1 (1995).
- ²⁶A. F. Voter and S. P. Chen, in *Characterization of Defects in Materials*, edited by R. W. Siegel, R. Sinclair, J. R. Weertman, MRS Symposia Proceedings Vol. 82 (Materials Research Society, Pittsburgh, 1987), p. 175.
- ²⁷M. S. Daw and M. I. Baskes, *Phys. Rev. B* **29**, 6443 (1984).
- ²⁸Y. Mishin, M. J. Mehl, D. A. Papaconstantopoulos, A. F. Voter, and J. D. Kress, *Phys. Rev. B* **63**, 224106 (2001).